Front. Biol. China 2009, 4(3): 321–327
DOI 10.1007/s11515-009-0027-4

RESEARCH ARTICLE

Preparation, characterization, and antibacterial activity of oleic acid-grafted chitosan oligosaccharide nanoparticles

Lu HUANG, Xiaojie CHENG, Chengsheng LIU, Ke XING, Jing ZHANG, Gangzheng SUN, Xiaoyan LI, Xiguang CHEN (✉)

College of Marine Life Science, Ocean University of China, Qingdao 266003, China

Abstract An oleic acid-grafted chitosan oligosaccharide (CSO-OA) with different degrees of amino substitution (DSs) was synthesized by the 1-ethyl-3-(3-dimethylaminopropyl) carbodiimide (EDC)-mediated coupling reaction. Fourier transform infrared spectroscopy (FT-IR) suggested the formation of an amide linkage between amino groups of chitosan oligosaccharide and carboxyl groups of oleic acid. The critical aggregation concentrations (CACs) of CSO-OA with 6%, 11%, and 21% DSs were 0.056, 0.042, and 0.028 $mg \cdot mL^{-1}$, respectively. Nanoparticles prepared with the sonication method were characterized by means of transmission electron microscopy (TEM) and Zetasizer, and the antibacterial activity against *Escherichia coli* and *Staphylococcus aureus* was investigated. The results showed that the CSO-OA nanoparticles were in the range of 60–200 nm with satisfactory structural integrity. The particle size slightly decreased with the increase of DS of CSO-OA. The antibacterial trial showed that the nanoparticles had good antibacterial activity against *E. coli* and *S. aureus*.

Keywords chitosan oligosaccharide, nanoparticles, antimicrobial activity

1 Introduction

Chitosan, poly[β-(1-4)-linked-2-amino-2-deoxy-D-glucose], is the N-deacetylated product of chitin, which is a major component of arthropod and crustacean shells such as lobsters, crabs, shrimps, and cuttlefishes. Chitosan and its derivatives have been identified as hydrophilic, nontoxic, biodegradable, antibacterial, and biocompatible and are widely accepted as active materials with antifungal activity (Hirano and Nagao, 1989; Kendra et al., 1989; Uchida et al., 1989; Roller and Covill, 1999; Ben-Shalom et al., 2003), antibacterial activity (Jeon and Kim, 2000; Choi et al., 2001; Helander et al., 2001; Liu et al., 2001; Chung et al., 2003), and antitumor activity (Suzuki et al., 1986; Koide, 1998; Mitra et al., 2001; Qin et al., 2002; Qin et al., 2004). Even though chitosan has very strong functional properties in many areas, its high molecular weight, high viscosity, and insolubility at physiological pH values (7.2–7.4) may restrict its uses *in vivo*.

However, the chitosan depolymerization products, i.e., low-molecular-weight chitosan (chitosan oligosaccharide, CSO), could overcome these limitations and hence find much wider applications in diversified fields (Vishu Kumar et al., 2004). With respect to antibacterial activity, chitosan oligosaccharide is superior to chitin since the former possesses a lot of polycationic amines, which interact with the negatively charged residues of macromolecules at the cell surface of bacteria (Young and Kauss, 1983) and subsequently inhibit the growth of bacteria. The antibacterial effect of chitosan oligosaccharide has been shown to be greatly dependent on the species of bacteria, concentration, pH, and so on. In addition, the water-soluble chitosan oligosaccharides may be advantageous as antibacterial agents in *in vivo* systems compared to water-insoluble chitosan. Chitosan oligosaccharide-based nanoparticles can be easily formed through self-aggregation. They have been synthesized as drug carriers as reported in previous studies and have also been employed as a gene carrier to enhance gene transfer efficiency in cells (Hu et al., 2006a, 2006b). However, the antibacterial activity of chitosan oligosaccharide nanoparticles has been seldom reported. The unique character of nanoparticles due to their small size and quantum size effect enables chitosan oligosaccharide nanoparticles to exhibit superior activities.

In this study, the oleic acid-grafted chitosan oligosaccharide (CSO-OA) copolymers with various degrees of amino substitution (DSs) were synthesized, and their

Received December 2, 2008; accepted January 6, 2009

E-mail: xgchen@ouc.edu.cn

molecular structures were analyzed by Fourier transform infrared spectroscopy (FT-IR). Nanoparticles were prepared using a sonication method. The morphology and size of nanoparticles were measured by transmission electron microscopy (TEM) and dynamic light scattering (DLS). *Escherichia coli* and *Staphylococcus aureus* were chosen to be models for the antibacterial assay of nanoparticles. The influences of DS of CSO-OA, concentration of the nanoparticles, and pH of the solution on the antibacterial activity of nanoparticles were also examined.

2 Materials and methods

2.1 Materials

Chitosan oligosaccharide (MW = 5 kDa), with a degree of deacetylation of 75%, was made from crab shell and obtained commercially. Oleic acid, pyrene, and 1-ethyl-3-(3-dimethylaminopropyl) carbodiimide (EDC) were purchased from Sigma Chemicals. All the other chemicals used in the study were of analytical grade.

2.2 Synthesis of CSO-OA

Oleic acid (OA) was coupled to CSO by the formation of amide linkages through the EDC-mediated reaction as described in a previous study (Liu et al., 2007). Briefly, CSO (1 g) was dissolved in 1% (w/v) aqueous acetic acid solution (100 mL) and diluted with 85 mL methanol. OA was added to CSO solution at 0.54 mol/L glucosamine residue of CSO followed by a drop-wise addition of 15 mL EDC methanol solution (0.07 g/L) while stirring at room temperature. The 1∶1 mol ratio of EDC to OA was used. After 24 h, the reaction mixture was poured into 200 mL of methanol/ammonia solution (7/3, v/v) while stirring. The precipitated material was filtered; washed with distilled water, methanol and ether; and then dried under vacuum for 24 h at room temperature. The DS, which can be defined as the number of OA groups per 100 amino groups of CSO, was evaluated according to the titration method (Smith et al., 1980).

The FT-IR spectra of CSO and CSO-OA were recorded on an FT/IR-430 Fourier Transform Infrared Spectrometer (Jasco Co. Tokyo, Japan) at room temperature based on the method of Shigemasa et al (1996). A pellet was formed from 2 mg of samples and 100 mg of KBr. Data analysis was carried out using Jwstda-32 (Windows xp).

2.3 Measurement of critical aggregation concentration

The critical aggregation concentration (CAC) was determined using pyrene as a fluorescence probe. Pyrene partitioned preferentially in the hydrophobic core of aggregates (micelles) and changed the photophysical properties of the micelles under investigation. Pyrene was first dissolved in acetone and then added to deionized water to a concentration of 5×10^{-7} mol/L. Acetone was subsequently removed by reducing the pressure and stirring for more than 5 h at 30°C. The concentration of CSO-OA in the water was varied from 0.0001 to 0.1 g/L. The pyrene and CSO-OA in the water were conjugated and equilibrated at room temperature for 1 day before measurement. The fluorescence spectra were obtained at room temperature using a fluorescence spectrophotometer (Shimadzu RF-5301PC). The fluorescence excitation spectra of pyrene were measured at a fixed emission wavelength (I_{em}) of 343 nm. The emission spectrum of pyrene was obtained at a fixed excitation wavelength (I_{ex}) of 390 nm.

2.4 Preparation of CSO-OA nanoparticles

Ten mg CSO-OA was suspended in 10 mL of phosphate buffered saline (PBS) buffer (pH 7.4), and the suspension was sonicated using a probe-type sonifier (Ultrasonic homogenizer UH-600) at 20 W in an ice bath. The sonication was repeated twice to get an optically clear solution using pulse function (pulse on, 10.0 s; pulse off, 2.0 s). The clear solution of nanoparticles was filtered to remove dust.

2.5 Characterization of CSO-OA nanoparticles

The morphology of the nanoparticles was observed by TEM with a JEM-2010. Solutions of CSO-OA nanoparticles were placed onto a copper grill covered with nitrocellulose. They were dried at room temperature and then were examined using TEM by negative staining with an aqueous solution of sodium phosphotungstate (Li et al., 2007).

The distribution size of nanoparticles was measured by DLS with a Zetasizer 3000. All DLS measurements were done at a wavelength of 632.8 nm and at 23°C.

2.6 Assays for antimicrobial activity

The antibacterial activity of CSO-OA nanoparticles was measured according to the method described by Xing (2008). The solution of CSO-OA nanoparticles (1000 mg/L) with different DSs was first prepared with 0.1 mol/L acetic acid, and then the pH was adjusted to 7.0 with 10% NaOH solution. The minimum inhibitory concentrations (MIC) of CSO-OA nanoparticles were determined by two-fold serial broth dilution (Qi et al., 2004), described above, and the optical density method. The control contained only nutrient broth and 0.1 mol·L^{-1} acetic acid without CSO-OA nanoparticles. After adjusting pH to 7.0 with 10% NaOH solution, all of the samples were inoculated under aseptic conditions with 50 μL of the inoculums of bacteria and incubated at 37°C for 24 h, and then the turbidity of the cultured medium was mensurated at 610 nm. The lowest

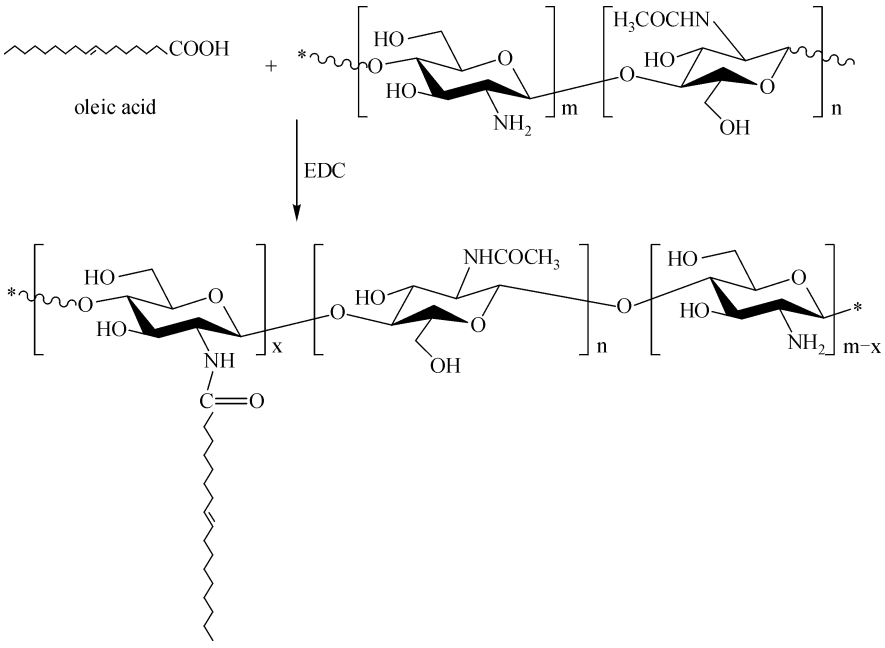

Fig. 1 Reaction scheme for the synthesis of the oleic acid-grafted chitosan oligosaccharide (CSO-OA). EDC: 1-ethyl-3-(3-dimethylaminopropyl) carbodiimide.

concentration of CSO-OA nanoparticles that inhibited the growth of bacteria was considered as the MIC. To examine the effect of pH, the pH of the solution of CSO-OA nanoparticles (1000 mg/L) with different DSs was adjusted to 4.0, 7.0, and 10.0 with 10% NaOH solution. The concentrations of both *E. coli* and *S. aureus* were adjusted to about 10^4 CFU/mL with sterile distilled water. Four mL CSO-OA nanoparticle solutions were added to 1 mL of the cell suspensions. The same volume of sterile distilled water was added to the control group. Samples were blended fully and removed after 5 min. Portions (50 μL) were spread on triplicate nutrient agar plates and incubated at 37°C for 24 h, and then the numbers of colonies were counted (Sudarshan et al., 1992; Choi et al., 2001).

2.7 Statistical analyses

The assays were performed at least in triplicate on separate occasions. The data collected were expressed as the mean values±standard deviation.

3 Results and discussion

3.1 Synthesis and characterization of CSO-OA

OA was covalently coupled to an amino group of CSO using EDC. Figure 1 shows the reaction scheme for the synthesis of the CSO-OA. CSO-OA was synthesized *via* the reaction of the carboxyl group of OA with the amino groups of CSO in the presence of water-soluble EDC. The remaining EDC could be easily removed by dialysis with water, and the remaining OA was washed with ethanol. A series of CSO-OAs with different DSs were obtained by changing the free mole ratios of OA to CSO. The DSs of CSO-OA were about 6%, 11%, and 21%, respectively, determined by a titration method.

Conjugation was confirmed by infrared spectrum (Fig. 2). Compared to the infrared spectroscopy (IR) spectrum of CSO, the spectra of CSO-OA exhibited many alterations: the absorption at 3000–3600 cm^{-1} (-OH, -NH_2) became weaker, and the vibrational band corresponding to primary amino groups at 1570 cm^{-1} decreased. The peaks

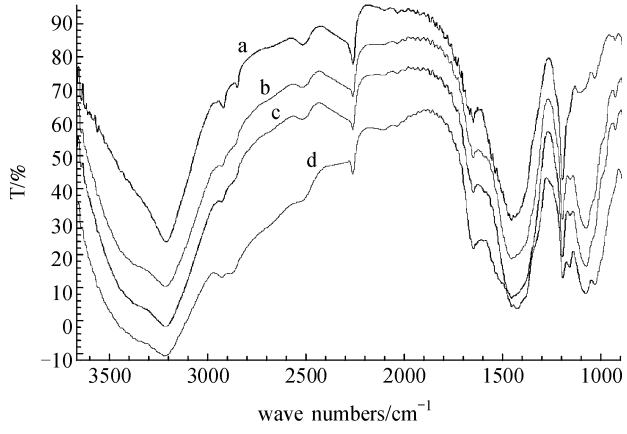

Fig. 2 Fourier transform infrared spectroscopy (FT-IR) of chitosan oligosaccharide (CSO) and oleic acid-grafted chitosan oligosaccharide (CSO-OA) with different degrees of amino substitution (DSs). a: CSO; b: CSO-OA with 6% DS; c: CSO-OA with 11% DS; d: CSO-OA with 21% DS. T: Transmittance.

at 2924 cm^{-1} ($\delta = CH_2$), 2854 cm^{-1} ($\delta = CH_2$), 1464 cm^{-1} ($\delta = CH_2$), and 1182 cm^{-1} (twisting vibration of CH_2) were stronger and sharper in the latter. These results confirmed that the CSO had been substituted with OA (Le Tien et al., 2003).

3.2 Formation of CSO-OA aggregation

The aggregation behavior of CSO-OA in aqueous media was investigated using a fluorometer in the presence of pyrene as a fluorescent probe. The fluorescence of pyrene is known to be sensitive to changes in the microenvironment. When the micelles are formed in an aqueous phase, pyrene molecules are preferentially located within or close to the hydrophobic microdomain of the micelles. Consequently, the photophysical characteristics of pyrene molecules in a hydrophobic surrounding differ obviously from those in an aqueous phase (Ananthapadmanabhan et al., 1985). Figure 3 plots the intensity ratio I_3/I_1 (I_{343}/I_{390}) for the pyrene excitation spectra versus the logarithm of CSO-OA concentration. The high-DS CSO-OA had a more pronounced hydrophobic character than the low-DS sample. The CAC values of the CSO-OA decreased with the increase in the content of hydrophobic OA because of the enhanced hydrophobicity. The CAC was determined from the crossover point in the low-concentration ranges. The CAC values determined in aqueous media were in the range of 0.056–0.028 mg/mL and decreased with increasing CSO-OA DS.

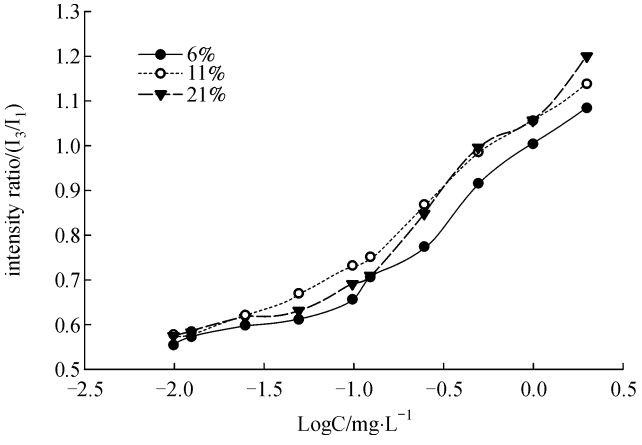

Fig. 3 Peak intensity ratio I_3/I_1 (I_{343}/I_{390}) of pyrene fluorescence as a function of oleic acid-grafted chitosan oligosaccharide (CSO-OA) with different degrees of amino substitution (DSs) in aqueous phase

3.3 Characterization of CSO-OA nanoparticles

The morphological characteristics of the CSO-OA nanoparticles were evaluated by a TEM. Figure 4 shows a TEM photograph of the CSO-OA nanoparticles dried at 25°C. The shapes of the CSO-OA nanoparticles were observed to be mostly spherical, and the range of diameters of these nanoparticles was about 60–100 nm when dehydrated. The size of self-aggregates decreased as the DS increased, indicating the formation of denser hydrophobic cores in high-DS samples. This was consistent with the fluorescence spectroscopic findings. These results indicated that the hydrophobically modified CSOs were well dispersed in aqueous media and that they formed a nanoparticle structure (Esquenet et al., 2004).

Based on the above results, CSO-OA with 6% DS was selected for further size distribution experiments. Figure 5 shows the size distribution of the nanoparticles formed by CSO-OA with 6% DS in the distilled water. The majority of particles were around 213 nm in size. The mean diameter and size distribution of self-aggregates appeared to be a little different from the results obtained by TEM measurement, primarily ascribed to the change of self-aggregates during the drying procedure for the preparation of TEM specimens; however, the general tendency was in good agreement.

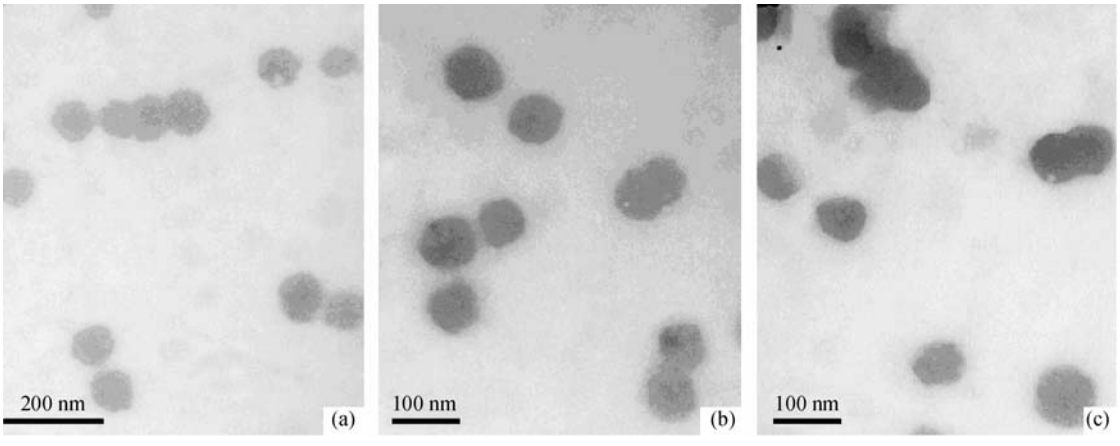

Fig. 4 Transmission electron microscopic photographs of oleic acid-grafted chitosan oligosaccharide (CSO-OA) nanoparticles, original magnification×30 000. a: with 6% DS; b: with 11% DS; c: with 21% DS.

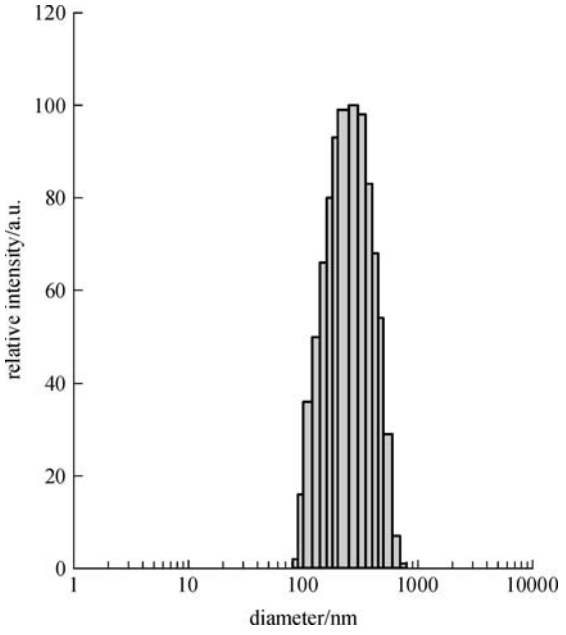

Fig. 5 Size distribution of oleic acid-grafted chitosan oligosaccharide (CSO-OA) nanoparticles with 6% degree of amino substitution (DS) of chitosan oligosaccharide (CSO)

3.4 Antimicrobial activity

3.4.1 Effect of concentration of nanoparticles on antibacterial activity

Figure 6 shows the effect of concentration on the antibacterial activity of CSO-OA nanoparticles against *E. coli* and *S. aureus*. As the concentrations ranged from 1.95 to 15.63 mg/L, the optical density (OD) values were not different between the experiment groups and control group for both bacteria. With the increase in the concentration, the antibacterial activities of the nanoparticle samples increased. When the concentration was higher than 62.5 mg/L for *S. aureus*, all nanoparticle samples showed their antibacterial activity obviously. When the concentration reached 250 mg/L, almost all bacteria were killed. Therefore, the MIC of all nanoparticle samples was 250 mg/L against *S. aureus*. For *E. coli*, when the nanoparticle concentrations were higher than 125 mg/L (sample C) and 250 mg/L (samples A and B), they could kill almost all of the bacteria. Thus, the MIC values of all nanoparticle samples were 125 mg/L (sample C) and 250 mg/L (samples A and B) against *E. coli*. These results indicated that the antibacterial activity increased as the concentration of nanoparticle samples increased, which was similar to its raw material CSO (Jeon and Kim 2000; Liu et al., 2001).

3.4.2 Effect of DS of CSO-OA on antibacterial activities

The effect of DS of CSO-OA on the antibacterial activity of nanoparticle samples against *E. coli* and *S. aureus* is also shown in Fig. 6. No marked difference was found among three nanoparticle samples tested in relation to *S. aureus*, while sample C formed by CSO-OA with 21% DS exhibited the most pronounced antibacterial activity against *E. coli*. The results indicated that the antibacterial activity increased as the DS of CSO-OA increased.

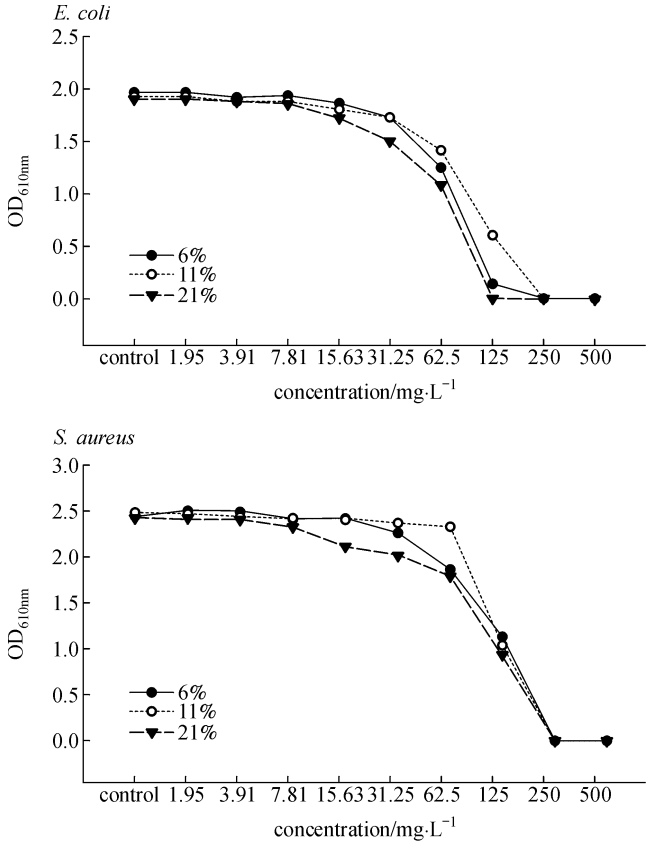

Fig. 6 Effect of concentration on the antibacterial activity of oleic acid-grafted chitosan oligosaccharide (CSO-OA) nanoparticles with different degrees of amino substitution (DSs) of chitosan oligosaccharide (CSO) against *E. coli* or *S. aureus*. OD: optical density.

3.4.3 Effect of different pH conditions on antibacterial activity

To examine the effect of pH on the antibacterial activity of nanoparticles, pH values of 4.0, 7.0, and 10.0 were selected. Figure 7 shows the effect of pH on the antibacterial activity of nanoparticles against *E. coli* and *S. aureus*. The antibacterial activity of nanoparticles increased upon increasing the pH of nanoparticles from 4.0 to 7.0 and decreased with further increase to 10.0 for both *E. coli* and *S. aureus*. All samples exerted complete inhibitory effects at pH 7.0, indicating that almost no bacteria existed under neutral condition. It was interesting to find that the antibacterial activity of nanoparticles in

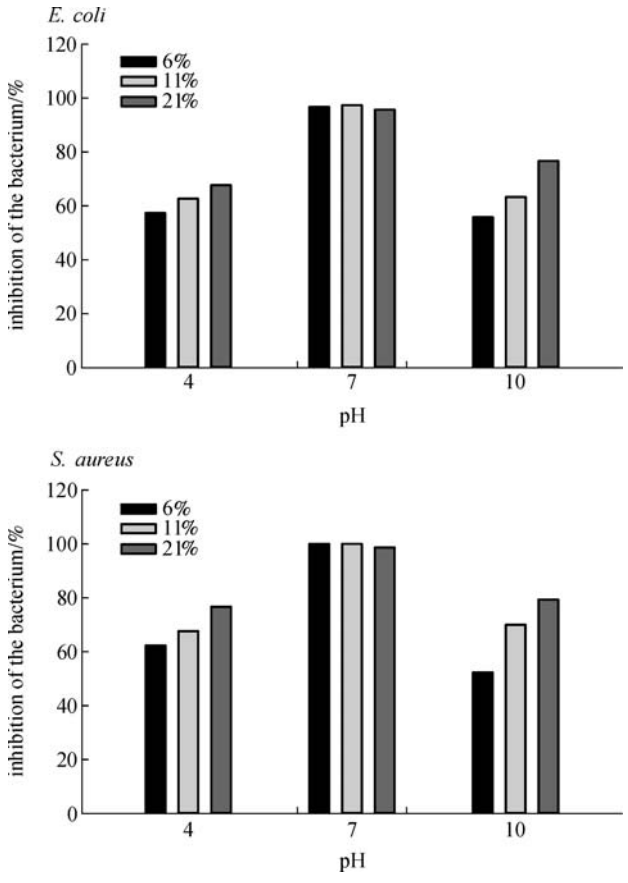

Fig. 7 Effect of pH on the antibacterial activity of oleic acid-grafted chitosan oligosaccharide (CSO-OA) nanoparticles with different degrees of amino substitution (DSs) of chitosan oligosaccharide (CSO) against *E. coli* or *S. aureus*

acidic and alkaline pH increased as the DS of CSO-OA increased. This result is consistent with Fig. 6. The nanoparticles with strong antibacterial activity at pH 7.0 could eliminate the effect of acetic acid on the bacterial growth greatly.

4 Conclusions

In summary, CSO-OA with different DSs was successfully synthesized. Due to their amphiphilic character, the hydrophobized CSOs could form nanoparticles in aqueous milieu easily. The mean diameters of the nanoparticles were in the range of 60–200 nm. The TEM images of nanoparticles showed a spherical shape. Taking *S. aureus* and *E. coli* as bacterial models, it was found that the antibacterial activity increased as the concentrations of nanoparticle samples and the DS of CSO-OA increased. Furthermore, the nanoparticles showed complete inhibitory effects at pH 7.0, indicating that almost no bacteria existed under neutral conditions. It is anticipated that CSO-OA nanoparticles could be applied broadly as antimicrobial agents in medicine for their high antibacterial activity and acceptable biocompatibilities.

Acknowledgements This work was supported by grants from the National Natural Science Foundation of China (Grant No. 30770582), the International S&T Cooperation Program of China (No. 2008DFA31640), and the Ph.D Programs Foundation of the Ministry of Education of China (No. 20070423013).

References

Ananthapadmanabhan K P, Goddard E D, Turro N J, Kuo P L (1985). Fluorescence probes for critical micelle concentration. Langmuir, 1 (3): 352–355

Ben-Shalom N, Ardi R, Pinto R, Aki C, Fallik E (2003). Controlling gray mould caused by *Botytis cinerea* in cucumber plants by means of chitosan. Crop Protection, 22(2): 285–290

Choi B K, Kim K Y, Yoo Y J, Oh S J, Choi J H, Kim C Y (2001). *In vitro* antimicrobial activity of a chitooligosaccharide mixture against *Actinobacillus actinomycetemcomitans* and *Streptococcus mutans*. International Journal of Antimicrobial Agents, 18(6): 553–557

Chung Y C, Wang H L, Chen Y M, Li S L (2003). Effect of abiotic factors on the antibacterial activity of chitosan against waterborne pathogens. Bioresource Technology, 88(3): 179–184

Esquenet C, Terech P, Boue F, Buhler E (2004). Structural and rheological properties of hydrophobically modified polysaccharide associative networks. Langmuir, 20(3): 3583–3592

Helander I M, Nurmiaho Lassila E L, Ahvenainen R, Rhoades J, Roller S (2001). Chitosan disrupts the barrier properties of the outer membrane of gram-negative bacteria. International Journal of Food Microbiology, 71(2,3): 235–244

Hirano S, Nagao N (1989). Effects of chitosan, pectic acid, lysozyme and chitinase on the growth of several phytopathogens. Agricultural and Biological Chemistry, 53(11): 3065–3066

Hu F Q, Ren G F, Yuan H, Du Y Z, Zeng S (2006). Shell cross-linked stearic acid grafted chitosan oligosaccharide self-aggregated micelles for controlled release of paclitaxel. Colloids and Surfaces B: Biointerfaces, 50(2): 97–103

Hu F Q, Zhao M D, Yuan H, You J, Du Y Z, Zeng S (2006). A novel chitosan oligosaccharide–stearic acid micelles for gene delivery: Properties and *in vitro* transfection studies. International Journal of Pharmaceutics, 315(1,2): 158–166

Jeon Y J, Kim S K (2000). Production of chitooligosaccharides using an ultrafiltration membrane reactor and their antibacterial activity. Carbohydrate Polymers, 41(2): 133–141

Kendra D F, Christian D, Hadwiger L A (1989). Chitosan oligomers from Fusarium solani/pea interactions, Chitinase/beta-glucanase digestion of sporelings and fungal wall chitin actively inhibit fungal growth and enhance disease resistance. Physiological and Molecular Plant Pathology, 35(3): 215–230

Koide S S (1998). Chitin-chitosan: Properties, benefits and risks. Nutrition Research, 18(6): 1091–1101

Le Tien C, Lacroix M, Ispas-Szabo P, Mateescu M A (2003). N-acylated chitosan: hydrophobic matrices for controlled drug release. Journal of Controlled Release, 93(1): 1–13

Li Y Y, Chen X G, Liu C S, Cha D S, Park H J, Lee C M (2007). Effect of the molecular mass and degree of substitution of oleoylchitosan on the structure, rheological properties, and formation of nanoparticles. Journal of Agricultural and Food Chemistry, 55: 4842–4847

Liu C G, Fan W W, Chen X G, Liu C S, Meng X H, Park H J (2007). Self-assembled nanoparticles based on linoleic-acid modified carboxymethyl-chitosan as carrier of adriamycin (ADR). Current Applied Physics, 7(Suppl 1): e125–e129

Liu X F, Guan Y L, Yang D Z, Li Z, Yao K D (2001). Antibacterial action of chitosan and carboxymethylated chitosan. Journal of Applied Polymer Science, 79(7): 1324–1335

Mitra S, Gaur U, Ghosh P C, Maitra A N (2001). Tumour targeted delivery of encapsulated dextran-doxorubicin conjugate using chitosan nanoparticles as carrier. Journal of Controlled Release, 74 (1-3): 317–323

Qi L F, Xu Z R, Jiang X, Hu C H, Zou X F (2004). Preparation and antibacterial activity of chitosan nanoparticles. Carbohydrate Research, 339(16): 2693–2700

Qin C Q, Du Y M, Xiao L, Zhan L, Gao X H (2002). Enzymic preparation of water-soluble chitosan and their antitumor activity. International Journal of Biological Macromolecules, 31(1-3): 111–117

Qin C Q, Zhou B, Zeng L T, Zhang Z H, Liu Y, Du Y M, Xiao L (2004). The physicochemical properties and antitumor activity of cellulase-treated chitosan. Food Chemistry, 84(1): 107–115

Roller S, Covill N (1999). The antifungal properties of chitosan in laboratory media and apple juice. International Journal of Food Microbiology, 47(1,2): 67–77

Shigemasa Y, Matsuura H, Sashiwa H, Saimoto H (1996). Evaluation of different absorbance ratios from infrared spectroscopy for analyzing the degree of deacetylation in chitin. International Journal of Biological Macromolecules, 18(3): 237–242

Smith P K, Mallia A K, Hermanson G T (1980). Colorimetric method for the assay of heparin content in immobilized heparin preparations. Analytical Biochemistry, 109(2): 466–473

Sudarshan N R, Hoover D G, Knorr D (1992). Antibacterial action of chitosan. Food Biotechnology, 6(3): 257–272

Suzuki K, Mikami T, Okawa Y, Tokoro A, Suzuki S, Suzuki M (1986). Antitumor effect of hexa-N-acetylchitohexaose and chitohexaose. Carbohydrate Research, 151: 403–408

Uchida Y, Izume M, Ohtakara A (1989). Preparation of chitosan oligomers with purified chitosanase and its application. In: Skjåk-Bræk G, Anthonsen T, Sandford P, eds. Chitin and chitosan: Sources, chemistry, biochemistry, physical properties and applications. London: Elsevier, 373–382

Vishu Kumar A B, Varadaraj M C, Lalitha R G, Tharanathan R N (2004). Low molecular weight chitosans: preparation with the aid of papain and characterization. Biochimica et Biophysica Acta-General Subjects, 1670(2): 137–146

Xing K, Chen X G, Li Y Y, Liu C S, Liu C G, Cha D S, Park H J (2008). Antibacterial activity of oleoyl-chitosan nanoparticles: A novel antibacterial dispersion system. Carbohydrate Polymers, 74(1): 114–120

Young D H, Kauss H (1983). Release of calcium from suspension cultured Glycine max cells by chitosan, other polycations, and polyamines in relation to effects on membrane permeability. Plant Physiology, 73: 698–702